Microscopic formulation of medium contributions to the first-order optical potential

C. R. Chinn
Department of Physics and Astronomy, Vanderbilt University, Nashville, Tennessee 37235
and Center for Computationally Intensive Physics, Oak Ridge National Laboratory, Oak Ridge, Tennessee 37831

Ch. Elster
Institute of Nuclear and Particle Physics and Department of Physics, Ohio University, Athens, Ohio 45701

R. M. Thaler
Department of Physics and Astronomy, Vanderbilt University, Nashville, Tennessee 37235
and Case Western Reserve University, Cleveland, Ohio 44106
(Received 28 July 1993)

A refinement of the first-order optical potential is introduced, consistent with multiple scattering theory and the spectator expansion. A systematic formalism is presented to treat medium contributions associated with the difference between the effective NN t matrix as required by multiple scattering theory and the free NN t matrix. A mean field potential is used to represent the action of the residual $(A-1)$ nucleus upon the struck target nucleon (medium effects). We calculate elastic proton and neutron scattering from ^{40}Ca, using the full Bonn interaction and two different mean field potentials taken from realistic and proven nuclear structure models. Results indicate that the medium contributions are insignificant at energies above 300 MeV and provide a significant improvement of the theoretical predictions for laboratory energies between 48 and 200 MeV.

PACS number(s): 24.10.Cn, 24.10.Ht, 25.40.Cm, 25.40.Dn

I. INTRODUCTION

The early successes of the first-order representation of the optical model potential derived from multiple scattering theories had been expected to be followed by illuminating higher-order studies which would yield significant new information about the nuclear force and various kinds of correlations in nuclei. Such expectations have not been realized. At this time improvements in the theory, in calculational techniques, and in the accuracy and availability of data suggest that such expectations may now be realistic. If higher-order studies are to be pursued in earnest, it is essential that the theory and understanding of the first-order calculations be completely reliable. Recent refinements of first-order multiple scattering theory calculations include, among others, (1) full-folding calculations, which incorporate the effects of the nonlocal density matrix [1–3]; (2) binding energy effects [4]; (3) exact treatment of the Coulomb potential in momentum space calculations [5, 6]; (4) second-order studies of Pauli effects [7]; (5) Coulomb exchange correction [8]; and (6) proper treatment of isospin [9].

In this work a further refinement of the first-order theory is introduced, which improves both the understanding of the multiple scattering process and the prediction of the data. In the first-order Watson [10] or Kerman-McManus-Thaler (KMT) [11] theory, the common practice has been to perform the standard "impulse approximation" in which the free nucleon-nucleon t matrix enters. This essentially entails the replacement of the many-body propagator with the free propagator. In this paper the difference between the many-body propagator and the free propagator is analyzed and modeled in a microscopic mean field approach. A formalism is developed as an extension to the first-order multiple scattering theory, where a mean field potential is used to represent the effects of the medium acting upon the target nucleon. Consistency with multiple scattering approaches, specifically the spectator expansion [12, 13], is maintained throughout. Since in this paper known quantities are used to represent the required physical ingredients, it must be emphasized that there are *no* adjustable parameters. Calculations are performed for ^{40}Ca. While the resulting effects are not large, they systematically improve the correspondence between calculation and measurement for both proton and neutron elastic scattering, especially when the projectile energy is below 200 MeV. With these new results the physical meaning of succeeding calculations should become clearer.

In the case of pion-nucleus scattering there exist some calculations which model medium effects by using simple one-body central potentials [14], based upon a formalism developed in Ref. [15]. In these calculations a set of three-body-like coupled equations are used to give the medium correction.

The theoretical derivation of the formalism is presented and discussed in Sec. II. The results are separated into three parts in Sec. III. In the first two parts elastic proton-nucleus and neutron-nucleus calculations are shown. The third part gives an analysis of the energy dependence of the nucleon-nucleon interaction as provided for in the formalism. The conclusion follows in Sec. IV.

II. THEORETICAL FRAMEWORK

The nucleon-nucleus multiple scattering formulation used in this paper is essentially that of Ref. [12], in which the Pauli principle is incorporated into the spectator expansion for the optical potential. This treatment of Pauli antisymmetry effects follows the philosophy growing out of the early work of Watson [10] and developed via the spectator expansion [12]. In the spectator expansion the transition operator, T, or the optical potential operator, $U_{\rm opt}$, is presented as a sum over n-body operators, where n goes from 2 to $A+1$, such that $T = \sum_{n=2}^{A+1} T_n$ or $U_{\rm opt} = \sum_{n=2}^{A+1} U_n$. In the lowest order the two-body antisymmetry is achieved through the use of two-body t matrices which are themselves antisymmetric in the two "active" variables. In the next order, the three-body t matrices which appear are taken to be antisymmetric with respect to the three "active" variables, and so on. The effect of the Pauli principle in the next order of this expansion has been estimated in Ref. [7] and found to be very small in the energy regime under consideration here.

The one-body transition operator for elastic nucleon-nucleus scattering is represented as

$$T = U_{\rm opt} + U_{\rm opt} G_0(E) P T, \tag{1}$$

where P is the projector onto the target ground state and $G_0(E)$ is the free propagator for the projectile-nucleus system defined as

$$G_0(E)^{-1} \equiv E - h_0 - H_A. \tag{2}$$

The energy E is the total energy of the $(A+1)$-body system, h_0 is the kinetic energy operator for the projectile nucleon and H_A is the target Hamiltonian. In the spectator expansion the lowest-order contribution to the optical potential becomes $U_{\rm opt} \approx \sum_{i=1}^{A} \tau_{oi}$, or $U_{\rm opt} \approx \tau\rho$, where ρ is the density of the target and τ_{oi} is given by

$$\tau_{oi} = v_{oi} + v_{oi} G_0(E) Q \tau_{oi}. \tag{3}$$

It should be noted that this is also the first-order term in the Watson expansion. In Eq. (3) v_{oi} is the two-body nucleon-nucleon interaction between the projectile nucleon "o" and the "i"th target constituent nucleon and $Q = 1 - P$ is the projector off the target ground state. As usual, it is assumed that there is complete antisymmetry among the target nucleons. It is also assumed that there exist only pairwise forces between the nucleons. The standard approximation to the first-order Watson or spectator expansion is the so-called "impulse approximation." This approximation is characterized by the substitution of the free two-body propagator $g_0(e)$ for the many-body propagator $G_0(E)$ in Eq. (3). In this way the operator τ of Eq. (3) becomes $\tau^{\rm IA}$, a two-body operator, which is related to the free $t_{oi}^{\rm free}$ as

$$\tau_{oi}^{\rm IA} = t_{oi}^{\rm free} - t_{oi}^{\rm free} g_0(e) P \tau_{oi}^{\rm IA}. \tag{4}$$

The difference between the use of $\tau_{oi}^{\rm IA}$ of Eq. (4) in place of τ_{oi} of Eq. (3) is the subject of the present investigation.

We have now to return to Eq. (2) to examine the relation between $G_0(E)$ and the free two-body propagator. We observe that H_A can be reexpressed as

$$H_A = h_i + \sum_{j\neq i}^{A} v_{ij} + H^i, \tag{5}$$

where H^i is the residual Hamiltonian involving the $(A-1)$ particles (exclusive of particles o and i), h_i is the kinetic energy operator for nucleon i, and v_{ij} is the interaction potential between target nucleons i and j. Clearly H_A is an A-body operator and hence $G_0(E)$ is an $(A+1)$-body operator. We then define a one-body Hamiltonian H_i as a particular average of H_A over the $(A-1)$ $j \neq i$ nucleons, such that

$$H_A \rightsquigarrow H_i \equiv h_i + U_i + \varepsilon^i, \tag{6}$$

where

$$U_i = \left\langle \sum_{j\neq i}^{A} v_{ij} \right\rangle \tag{7}$$

and

$$\varepsilon^i = \langle H^i \rangle \ . \tag{8}$$

The mean field potential U_i is a one-body operator and ε^i is a c number (an energy shift). At this point any discussion of the averaging process implied by the '$\langle\ \rangle$' symbol is postponed, and the crucial theoretical question involving the treatment of $(\sum_{j\neq i}^{A} v_{ij} + H^i - U_i - \varepsilon^i)$ is deferred until later. After these averages are taken, the propagator, $G_0(E)$, becomes

$$\begin{aligned} G_0(E_i, i)^{-1} &= (E - \varepsilon^i) - h_0 - h_i - U_i \\ &= E_i - h_0 - h_i - U_i. \end{aligned} \tag{9}$$

The energy, E_i, is

$$\begin{aligned} E_i &= E - \varepsilon^i = E - [\varepsilon^i + \varepsilon_i] + \varepsilon_i \\ &= E + \varepsilon_i, \end{aligned} \tag{10}$$

where ε_i is the ith nucleon's single-particle energy and $\varepsilon^i + \varepsilon_i = \langle H_A \rangle$ is chosen to be zero. The propagator $G_0(E_i, i)$ is a two-body operator and the operator

$$\tilde{t}_{oi} = v_{oi} + v_{oi} G_0(E_i, i) \tilde{t}_{oi} \tag{11}$$

is likewise a two-body operator.

The operator $\tilde{t}_{oi}$ will be related to the free nucleon-nucleon t matrix on the one hand, and on the other hand to the operator, $\tilde{\tau}_{oi}$, defined as

$$\tilde{\tau}_{oi} = v_{oi} + v_{oi} Q G_0(E_i, i) Q \tilde{\tau}_{oi}, \tag{12}$$

where $\tilde{\tau}\rho$ will represent the lowest-order approximation to the optical potential [Eq. (3)].

By elimination of v_{oi} between Eqs. (11) and (12) above,

$$\tilde{\tau}_{oi} = \tilde{t}_{oi} - \tilde{t}_{oi} P G_0(E_i, i) P \tilde{\tau}_{oi} \tag{13}$$

is obtained. The operator of interest is $P\tilde{\tau}_{oi}P$, since $P\sum_i^A \tilde{\tau}_{oi} P$ corresponds to the one-body optical potential operator in the first-order theory. The operator $P\tilde{\tau}_{oi}P$ is easily obtained as a solution of the one-body integral equation

$$(P\tilde{\tau}_{oi}P) = (P\tilde{t}_{oi}P) - (P\tilde{t}_{oi}P) G_0(E_i, i) (P\tilde{\tau}_{oi}P). \tag{14}$$

Next $\tilde{t}_{oi}$ may be written in terms of t_{oi}^{free}, since

$$t_{oi}^{\text{free}} = v_{oi} + v_{oi} g_0(e) t_{oi}^{\text{free}}, \tag{15}$$

with

$$g_0(e)^{-1} = e - h_0 - h_i. \tag{16}$$

The obvious relationship between $\tilde{t}_{oi}$ and t_{oi}^{free} is then

$$\tilde{t}_{oi} = t_{oi}^{\text{free}}(e) + t_{oi}^{\text{free}}(e)[G_0(E_i, i) - g_0(e)]\tilde{t}_{oi}, \tag{17}$$

where the parametric energy e is as yet undefined. The difference between G_0 and g_0 corresponds to the medium effect under discussion in this work. This is the only such effect included in the first-order theory, as discussed at length in Ref. [12]. It is, of course, possible to take a different attitude toward the manner in which one includes the projectile-target antisymmetrization in the multiple scattering expansion (cf. Ref. [16]). The present treatment is a direct descendant of that first proposed by Takeda and Watson [17].

The quantity, $G_0(E_i, i) - g_0(e)$ can be rewritten as

$$\begin{aligned} G_0(E_i, i) - g_0(e) &= G_0(E_i, i)[g_0(e)^{-1} - G_0(E_i, i)^{-1}] g_0(e) \\ &= G_0(E_i, i)[e - h_0 - h_i - E_i + h_0 + h_i + U_i] g_0(e) \\ &= G_0(E_i, i) U_i g_0(E_i) \\ &= g_0(E_i) \mathcal{T}_i(E_i) g_0(E_i), \end{aligned} \tag{18}$$

where we have chosen $e = E_i$ for obvious reasons. The operator $\mathcal{T}_i(E_i)$ is, of course, the transition operator corresponding to the internal target potential U_i, i.e.,

$$\mathcal{T}_i(E_i) = U_i + U_i g_0(E_i) \mathcal{T}_i(E_i) \ . \tag{19}$$

The effective nucleon-nucleon t matrix $\tilde{t}_{oi}$ becomes

$$\begin{aligned} \tilde{t}_{oi} &= t_{oi}^{\text{free}}(E_i) + t_{oi}^{\text{free}}(E_i) g_0(E_i) \mathcal{T}_i(E_i) g_0(E_i) \tilde{t}_{oi} \\ &= t_{oi}^{\text{free}}(E_i) + w_{oi}(E_i) g_0(E_i) \tilde{t}_{oi}, \end{aligned} \tag{20}$$

with $w_{oi}(E_i)$ defined to be

$$w_{oi}(E_i) \equiv t_{oi}^{\text{free}}(E_i) g_0(E_i) \mathcal{T}_i(E_i). \tag{21}$$

It then proves convenient to rewrite Eq. (20) as

$$\tilde{t}_{oi} = t_{oi}^{\text{free}} + \Delta_{oi}, \tag{22}$$

so that

$$\Delta_{oi} \equiv t_{oi}^{\text{free}} g_0(E_i) \eta_{oi}(E_i), \tag{23}$$

with η_{oi} given by

$$\eta_{oi}(E_i) = w_{oi}(E_i) + w_{oi}(E_i) g_0(E_i) \eta_{oi}(E_i) \ . \tag{24}$$

The formal derivation implied by Eqs. (1)–(24) can be realized in the following set of steps.

(1) Find or choose a mean field potential to represent U_i.

(2) Solve the integral equation, Eq. (19), for $\mathcal{T}_i(E_i)$.

(3) Construct $w_{oi}(E_i)$ using Eq. (21).

(4) Solve the integral equation, Eq. (24), for $\eta_{oi}(E_i)$.

(5) Construct Δ_{oi} using Eq. (23).

(6) Add Δ_{oi} to t_{oi}^{free} to obtain $\tilde{t}_{oi}$, cf. Eq. (22).

(7) Take matrix elements of the effective nucleon-nucleon t matrix, $\tilde{t}_{oi}$ using target nucleus wave functions (i.e., folding $\tilde{t}_{oi}$ with the nuclear density matrix).

(8) Solve the implied one-body integral equation, Eq. (13), for $\tilde{\tau}_{oi}$.

(9) Obtain the first-order opt model potential $U_{\text{opt}} = \sum_i^A P \tilde{\tau}_{oi} P$; i.e., $U_{\text{opt}} = \tilde{\tau}\rho$.

(10) Solve the one-body Lippmann-Schwinger equation, Eq. (1), for T, the nucleon-nucleus transition operator for elastic scattering.

It is noted that although $G_0(E)$ is a complicated many-body operator, the operator $G_0(E)\,P$, which appears in Eq. (1) is the trivial one-body operator, $G_0(E)\,P = (E + i\epsilon - h_0)^{-1} P$.

An alternate approach to a calculation of a medium correction is presented in Ref. [15], where a set of coupled three-body integral equations are derived to give Δ_{oi}. This method has been applied to pion-nucleus scattering [14], where local, central square-well and Woods-Saxon potentials were used to represent the interaction between the target nucleon and the residual nucleus.

The formalism presented here should be differentiated from other approaches in the field of nucleon-nucleus scattering. Specifically, models exist which attempt to represent a medium correction through the introduction of a Fermi gas Pauli blocking operator within a local density approximation of nuclear matter to derive an effective nucleon-nucleon (NN) t matrix [18, 19]. Although, a degree of success can be attributed to the results obtained in these other approaches, a cleaner and more precise understanding of the physical interpretation and construction of medium effects is called for. In contrast, in the present approach familiar quantities can be taken from realistic and proven nuclear structure calculations and nucleon-nucleon scattering to model the medium contributions, while consistency with multiple scattering theory and the spectator expansion is maintained.

The above step-by-step treatment is a straightforward, precise formulation of the procedure for the calculation of the elastic optical potential in lowest order in the spectator expansion. In practice, however, the ten steps outlined above are awkward to realize, because the operator, $w_{oi}(E_i)$ (step 3) is an operator in the variables $(\vec{k}_o', \vec{k}_i', \vec{k}_o, \vec{k}_i)$, which does *not* separate into the two-body form $w_{oi} = \delta[(\vec{k}_o' + \vec{k}_i') - (\vec{k}_o + \vec{k}_i)] \times w_{oi}(\vec{k}_o' - \vec{k}_i', \vec{k}_o - \vec{k}_i)$. This is, of course, the form which all Galilean-invariant two-body operators take, so that two-body equations can be reduced to effective one-body equations. In order to facilitate calculations we approximate w_{oi} in such a fashion that it does so factorize into a pair-momentum conserving delta function and a function of the relative momenta. The rationale for such an approximation to w_{oi} follows.

Equation (21) can be written in momentum space as

$$\langle \vec{k}_o', \vec{k}_i' | w | \vec{k}_o, \vec{k}_i \rangle = \int \frac{\delta(\vec{p}' - \vec{p}'') t_{oi}^{\text{free}}(\vec{q}_i\,', \vec{q}_i\,'') \delta(\vec{k}_o'' - \vec{k}_o) \mathcal{T}_i(\vec{k}_i'' - \vec{k}_i)}{E_i - h_0(\vec{k}_o'') - h_i(\vec{k}_i'') + i\epsilon} d^3\vec{k}_o''\, d^3\vec{k}_i''$$
$$= \int \frac{\delta(\vec{p}' - \vec{p}'') t_{oi}^{\text{free}}(\vec{q}_i\,', \vec{q}_i\,'') \delta(\vec{k}_o'' - \vec{k}_o) \mathcal{T}_i[(\vec{k}_i'' - \vec{k}_o'') - (\vec{k}_i - \vec{k}_o)]}{E_i - h_0(\vec{k}_o'') - h_i(\vec{k}_i'') + i\epsilon} d^3\vec{k}_o''\, d^3\vec{k}_i'', \tag{25}$$

where h_i is the kinetic energy operator for particle i and where, to simplify the argument, we have taken $\mathcal{T}_i$ to be local. It is to be noted that the choice of $\mathcal{T}_i$ as local is for clarity alone and is not essential. The variables $\vec{p}$ and $\vec{q}_i$ are defined as $\vec{p} = \vec{k}_o + \vec{k}_i$ and $\vec{q} = \frac{1}{2}(\vec{k}_i - \vec{k}_o)$, so that in terms of these variables Eq. (25) becomes

$$\langle \vec{k}_o', \vec{k}_i' | w | \vec{k}_o, \vec{k}_i \rangle = \int \frac{\delta(\vec{p}' - \vec{p}'') t_{oi}^{\text{free}}(\vec{q}_i\,', \vec{q}_i\,'') \delta[\frac{1}{2}(\vec{p}'' - \vec{p}) - (\vec{q}_i\,'' - \vec{q}_i)] \mathcal{T}_i(\vec{q}_i\,'' - \vec{q}_i)}{E_i - \frac{1}{2}h(\vec{p}'') - \frac{1}{2}h(\vec{q}_i\,'') + i\epsilon} d^3\vec{p}''\, d^3\vec{q}_i\,''. \tag{26}$$

For sufficiently large nuclei, $\mathcal{T}_i$ is long ranged (in coordinate space), especially as compared to the short-ranged free nucleon-nucleon t matrix, t_{oi}^{free}. Since Eq. (26) involves a folding of $\mathcal{T}_i$ with the short-ranged t_{oi}^{free}, in the region where the integrand is large $\mathcal{T}_i$ should be approximately constant in coordinate space. If $\mathcal{T}_i$ were infinitely long ranged, then it would be represented by a delta function in momentum space, so that the delta function $\delta[(\vec{p}'' - \vec{p}) - (\vec{q}_i\,'' - \vec{q}_i)]$ would become $\delta(\vec{p}'' - \vec{p})$. With this in mind Eq. (26) can be approximated as

$$\langle \vec{k}_o', \vec{k}_i' | w | \vec{k}_o, \vec{k}_i \rangle = \delta(\vec{p}' - \vec{p}'') 2^3 \int \frac{t_{oi}^{\text{free}}(\vec{q}_i\,', \vec{q}_i\,'') \mathcal{T}_i(\vec{q}_i\,'' - \vec{q}_i)}{E_i - \frac{1}{2}h(\vec{p}'') - \frac{1}{2}h(\vec{q}_i\,'') + i\epsilon} d^3\vec{q}_i\,''. \tag{27}$$

The approximation given in Eq. (27) is that used in these calculations. In that case, the momentum conserving delta function $\delta(\vec{p}' - \vec{p}'')$ factors out of the integral and the remaining steps (4–10) are integrals or integral equations involving only the relative momenta of the projectile and target nucleon. Without this approximation, it would be necessary to account for the recoil of the residual $A - 1$ nucleus via the solution of a six-dimensional integral equation instead of a three-dimensional equation. The accuracy of this approximation has not been tested, but we are confident that this is a reasonable procedure for heavier nuclei.

III. RESULTS

Step 1 involves choosing a model to represent the average mean field potential, U_i, which is felt by the ith target nucleon. It would be ideal to construct U_i from the same nucleon-nucleon interaction, which is used to construct the free nucleon-nucleon t matrix. The problem though is that it has been shown, through numerous attempts to construct (via, for example, Brueckner theory) the nuclear mean field using accurate representations of the free nucleon-nucleon interaction, that such approaches fail to provide realistic and accurate descriptions of nuclear structure and nuclear matter [20]. Hence the choice is made here to incorporate realistic and proven nuclear mean field models to represent U_i, models which utilize effective nucleon-nucleon interactions.

Two different mean field potentials are used in our calculations, so as to isolate any model dependence which may exist. One is the nonlocal nonrelativistic mean field potential taken from a Hartree-Fock-Bogolyubov microscopic nuclear structure calculation, which utilizes the density-dependent finite-ranged Gogny D1S nucleon-nucleon interaction [21, 22]. This model formalism has been shown to provide realistic, accurate representations of a variety of nuclear structure effects. Calculations using this potential to model the medium effects will be referred to as HFB. The second choice involves a nonrelativistic reduction of the mean field potentials resulting from a Dirac-Hartree calculation based upon the σ-ω model [23]. The calculations with this potential will in turn be referred to as DH. Comparisons of calculations with these two models may isolate the medium effects, as well as indicate any dependence upon the model used to construct the nuclear mean field potential.

The full Bonn potential [24] is used to calculate the free nucleon-nucleon interaction, t_{oi}^{free} for projectile energies less than 300 MeV. This interaction includes the effects of relativistic kinematics, retarded meson propagators as given by time-ordered perturbation theory, and crossed and iterative meson exchanges with NN, $N\Delta$, and $\Delta\Delta$ intermediate states. For energies greater than 300 MeV a high-energy extension of the Bonn potential [25], which incorporates the effects of pion production, is used.

The series of equations described in steps 1–6 are projected upon a helicity basis, which allows for the full angular momentum content of the theory to be included. Hence, the effects due to the spin-orbit term in U_i and the spin structure of t_{oi}^{free} are treated explicitly. With the approximation embodied by Eq. (27) each of these equations reduces to a set of one-dimensional equations. The helicity basis, as applied to two-body integral equations, is described in detail in Refs. [24, 26].

Step 7 is approximated using the optimum factorization approximation as described in Ref. [27], where the fully off-shell effective t matrix, $\tilde{t}_{oi}$, is used, but with the diagonal density. The full folding of the off-shell t matrix and the fully nonlocal density matrix has been shown to give significant effects using model wave functions. The proton densities are taken from electron scattering [28], while the neutron densities are those calculated from the Hartree-Fock-Bogolyubov calculation described above [21].

Steps 8–10 are straightforward one-body integral equations which are solved in partial wave form. The effects of the Coulomb interaction in the case of proton scattering

are included nonrelativistically using an exact method as described in Refs. [5, 6]. All of the calculations in this paper are performed in momentum space. Therefore, the medium correction and the description of the nucleon-nucleon interactions include the nonlocal and off-shell effects.

The results for the calculations shown in the following sections are for scattering from ^{40}Ca, which is doubly magic and spin saturated. By assuming a spin saturated target, only the spin-independent and spin-orbit terms of the effective t matrix $\tilde{t}_{oi}$ need be included in step 7. The calculations used to generate the results presented in Secs. III A and III B assume that E_i as defined in Eq. (9) is equal to E. It is found that the nucleon-nucleus scattering results are rather insensitive to changes in E. Effects due to the difference between E_i and E are shown in Sec. III C.

A. Proton-nucleus scattering results

In Figs. 1–6, 10, and 11 elastic scattering calculations of the angular distribution of the differential cross section, analyzing power A_y, and spin rotation parameter Q are shown, where the solid curves correspond to the use of the free off-shell NN t matrix, $t_{oi}^{\rm free}(E)$ in place of the off-shell operator, $\tilde{t}_{oi}$, in step 7, and will be referred to as the free result. The solid curves correspond to the standard impulse approximation to the optical potential, in which no medium contributions are included [$t_{oi}^{\rm free}(E)$ replaces $\tilde{t}_{oi}$ in step 7]. The dashed curves include the full medium contributions corresponding to steps 1–6. Use of the local DH potential to represent the mean field, U_i, acting upon the target nucleon gives the short-dashed lines and the corresponding calculation using the nonlocal HFB potential gives the long-dashed lines.

It is generally expected that the first-order impulse approximation is valid for projectile kinetic energies T_p greater than ~200 MeV. Our calculations for T_p = 200 MeV are displayed in Fig. 1. The solid line represents the result obtained with the free NN t matrix, the dashed lines include the modifications due to the nuclear medium. The two medium results are very similar and it can be said that there appears to be little model dependence on the manner in which U_i is represented. This is true for all of the cases studied. In contrast to expectations that any complicated higher-order processes would cause the diffraction pattern in the differential cross section to be less distinct, what is found instead is that although the medium has a small effect upon the differential cross section, at T_p = 200 MeV it causes the minima to be deeper and also shifts them to higher scattering angles. For the spin observables the medium is non-negligible causing the analyzing power to have deeper minima at slightly larger angles, where at the first minimum the theoretical curves are actually moved significantly closer to the data. The spin rotation parameter, Q, does not favor any one of the curves over the other.

The medium contributions should become more important at lower projectile energies. In Fig. 2, where T_p = 160 MeV, effects similar to those seen in Fig. 1

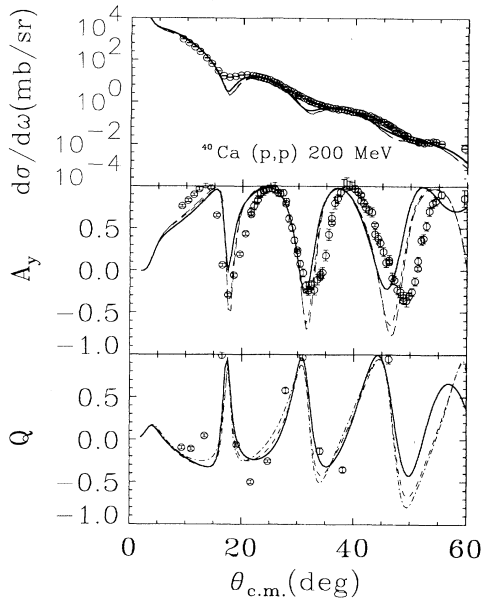

FIG. 1. The angular distribution of the differential cross section ($\frac{d\sigma}{d\Omega}$), analyzing power (A_y), and spin rotation function (Q) for elastic proton scattering from ^{40}Ca at 200 MeV laboratory energy. The calculations are performed with a first-order optical potential obtained from the full Bonn interaction [24] in the optimum factorized form. The solid curve represents the free impulse approximation using the free NN t matrix in step 7. The medium contributions are included in the dashed curves, where the DH mean potential is used for the short-dashed curve and the HFB mean field potential for the long-dashed curve. The data are taken from Ref. [32].

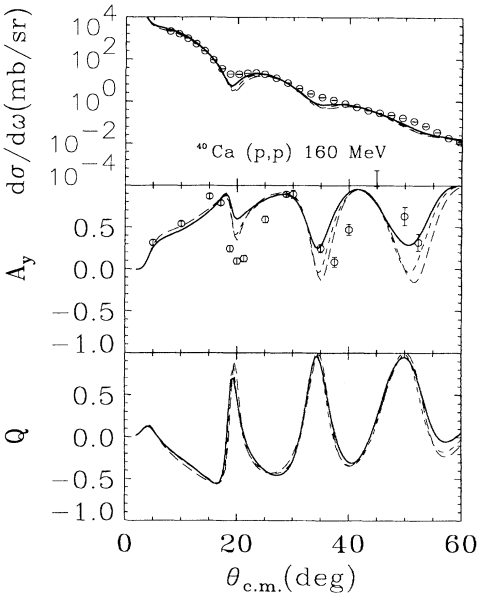

FIG. 2. Same as Fig. 1, except the projectile kinetic energy is 160 MeV and the data are taken from Ref. [33].

result. The diffraction pattern for the differential cross section and A_y are slightly deeper and shifted to larger angles, so that it might be said that the incorporation of medium effects makes the nucleus appear slightly more compact. The medium contribution brings the structure of the A_y closer to the data, although there still exists some lack of agreement. Again little effect is seen in Q. In Fig. 3 at $T_p = 100$ MeV a ledge appears in the A_y data at angles $10° - 20°$. While the medium has a small effect in the differential cross section, the A_y is systematically brought closer to the data. The ledge is clearly better represented when the effects due to the medium are included. In addition the spin rotation parameter is reduced, but there are no data for comparison.

It is felt that the first-order multiple scattering expansion should begin to become inadequate at energies less than 200 MeV, and should have serious flaws at energies less than about 100 MeV. While no claims are made about the validity of the first-order multiple scattering theory, studies of the medium contribution are presented in Figs. 4–6 for $T_p \leq 80$ MeV. The effects become more important at these lower values of the projectile kinetic energy. In Fig. 4, where $T_p = 80$ MeV, the medium contribution now causes the minima in the differential cross section sometimes to be less deep. The shift to higher angles is more pronounced than that observed in the previous figures. It is clear that although the agreement with the data remains imperfect, the medium contribution brings the differential cross section closer to the data. The ledge in the A_y is deeper than that seen in Fig. 3. The prediction of A_y is even more improved than what was observed at $T_p = 100$ MeV, providing a better representation of the ledge and likewise shifts the peaks towards the data. There is a larger shift downward of the spin rotation than observed in Fig. 3. At $T_p = 65$ MeV in Fig. 5 the medium enhances the differential cross section

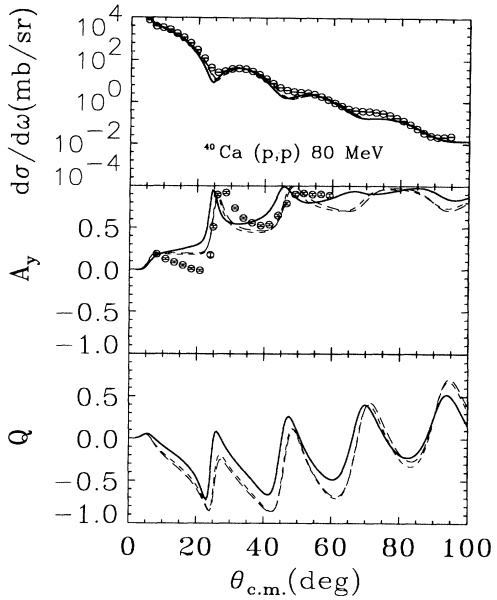

FIG. 4. Same as Fig. 1, except the projectile kinetic energy is 80 MeV and the data are taken from Ref. [33].

towards the data improving the agreement with the data. The ledge in the A_y is more pronounced than at higher T_p, and the medium contribution continues to improve the prediction. There is a significant improvement in the description of the ledge. The data between 35° and 55° is missed by the solid curve, but the dashed curves provide excellent agreement with the data. At this energy there exists spin rotation data. The medium shifts the Q downward significantly and at angles less than 60°, this shift results in excellent agreement with the data. Fig-

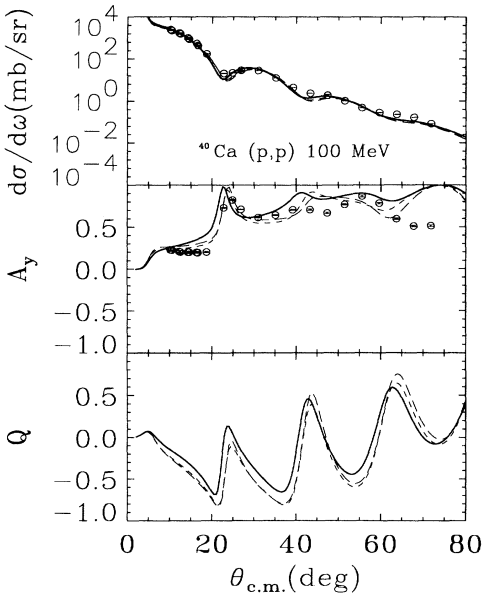

FIG. 3. Same as Fig. 1, except the projectile kinetic energy is 100 MeV and the data are taken from Ref. [34].

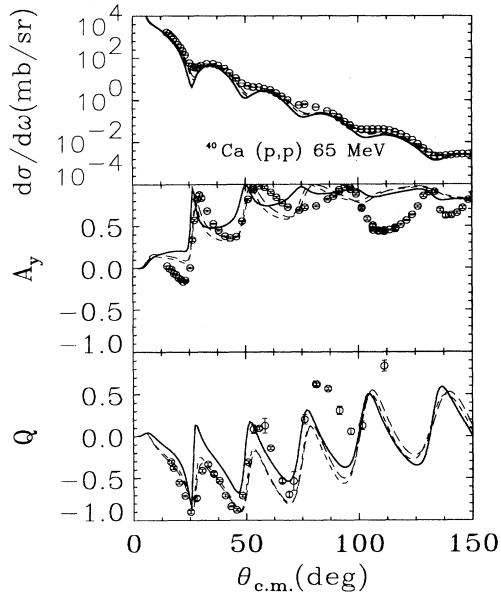

FIG. 5. Same as Fig. 1, except the projectile kinetic energy is 65 MeV and the data are taken from Ref. [35].

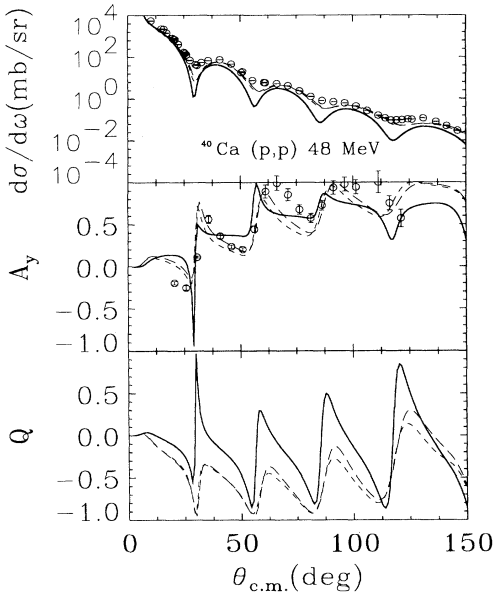

FIG. 6. Same as Fig. 1, except the projectile kinetic energy is 48 MeV and the data are taken from Ref. [36].

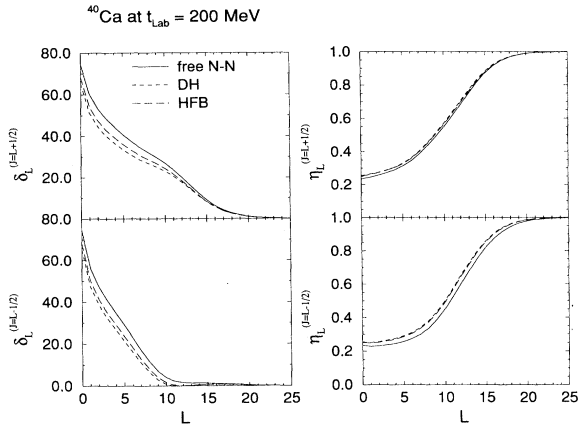

FIG. 7. The real part of the phase shift δ_L and the absolute value of the S-matrix η_L are shown as functions of the orbital angular momentum L for scattering from ^{40}Ca at 200 MeV laboratory energy. The solid line is the free result, while the short- and long-dashed lines include the medium contributions using the DH and HFB mean field potentials, respectively.

ure 6 contains results at $T_p = 48$ MeV, where it can be seen that the medium effect shifts significantly the differential cross section predictions towards the data. The shape of the A_y is modified by the medium to provide better agreement with the data for angles less than 60°.

It is clear from Figs. 1–6 that the medium contribution as represented in our model provides a systematic and significant improvement of the theoretical predictions of the data. The improved agreement with the data becomes systematically better as the kinetic energy of the projectile is reduced. In the parameter-free, *a priori* formalism derived here it is found that the resulting calculated effects are important in providing better agreement with the data.

To illustrate the effects of the medium contribution in more detail, the real part of the phase shifts, δ_L, along with absolute values of the S matrix, η_L, are shown as functions of the orbital angular momentum, L. The $J = L + \frac{1}{2}$ and $J = L - \frac{1}{2}$ cases are separated to display any spin-orbit effects. The results with $T_p = 200$ and 100 MeV are shown in Figs. 7 and 8, respectively. In comparing these two figures the phase shifts are decreased significantly by the medium. At $T_p = 200$ MeV the medium causes a reduction of δ_L for $L \lesssim 15$, where $\delta_L^{(J=L-1/2)}$ for $L = 11, 12$ is actually negative. This reduction exists for $L \lesssim 10$, where $T_p = 100$ MeV. The large changes in the real part of the phase shifts as shown in Figs. 7 and 8 are not particularly relevant because of the strong absorption, as is evident from the plots of η_L, also given in those figures. This strong absorption also implies strong surface effects as well as weak interior contributions and causes the higher partial waves to play an exaggerated role in elastic nucleon-nucleus scattering. The medium contributions have a significant effect on the absorption, especially as the energy decreases, as is illustrated in Figs. 7 and 8. We see a uniform decrease in the absorptive character of the potential for all angular momenta, L, which is reflected in the shifted diffraction pattern of the observables described earlier.

B. Neutron-nucleus scattering results

In this section comparisons are made between theoretical predictions and measurements of the total cross section for neutron-nucleus scattering. For the case where the impulse approximation is used and no medium contributions are included, the theoretical calculations did not provide a very good prediction of the data as can be seen in Fig. 9. The results which come from the use of $t_{oi}^{\text{free}}(E)$ with no medium contribution are given by the circles. The medium inclusion from the DH potential and the HFB potential are represented by the squares and tri-

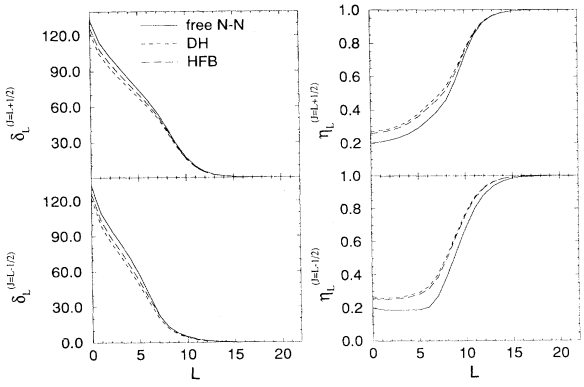

FIG. 8. The same as Fig. 7, except the laboratory energy is 100 MeV.

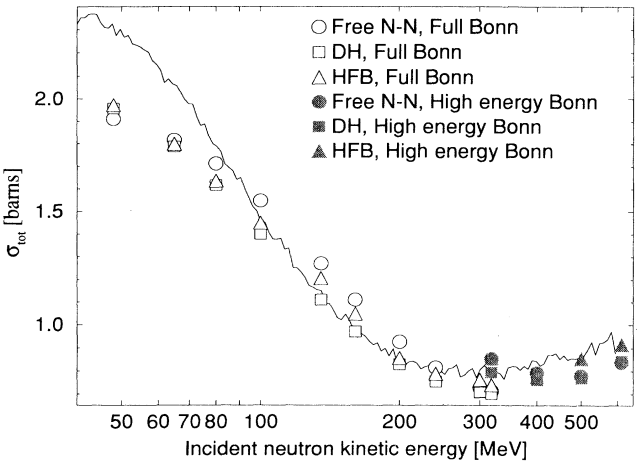

FIG. 9. The total neutron-nucleus total cross sections for scattering from ^{40}Ca are shown as a function of the incident neutron kinetic energy. The solid line represents the data taken from Refs. [29, 30]; the error bars are too small to display. The circles correspond to the free result, while the squares and triangles include the medium contributions using the DH and HFB mean field potentials, respectively. The open symbols indicate use of the full Bonn NN t matrix [24], while the shaded symbols are for the high energy extension of the Bonn potential [25].

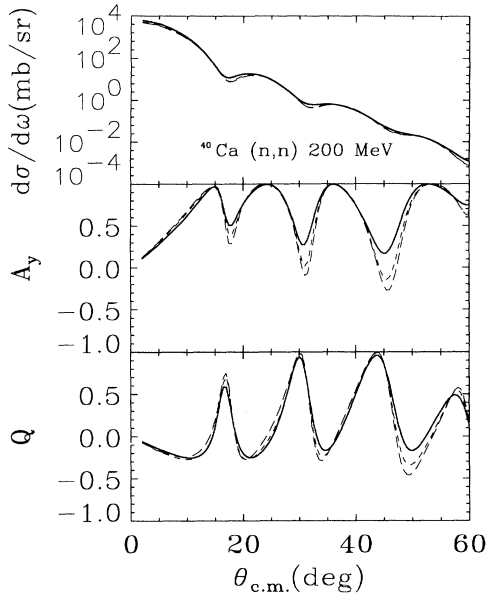

FIG. 10. The same as Fig. 1, except this is for elastic neutron-nucleus scattering at 200 MeV laboratory energy.

angles, respectively. The open symbols correspond to use of the full Bonn potential [24], while the filled symbols come from the high-energy extension above pion threshold [25]. The data are given by the solid line; the error bars have been omitted since they are very small [29, 30]. For energies between 100 and 200 MeV the free case overestimates the data and for energies above 400 MeV the free case underestimates the data.

The medium contribution causes the theoretical predictions to improve in both of these energy regions. For incident neutron kinetic energies between 100 and 200 MeV the medium decreases the total cross section towards the data, while at 500 and 613 MeV the medium increases the theoretical result toward the data. The effect of the medium contribution is to provide significant improvement of the predictions and generally results in good agreement with the experimental measurements. It is interesting to note that the improvement in the predictions of the total cross section due to the medium contribution is not a general overall reduction or increase, but comes about through a reduction in one energy region and an increase in another.

Since the systematic increase in one energy range and decrease in another also corresponds to the two model representations of the NN potential, it was verified at lower energies that the qualitative features of these medium effects are dependent on the projectile energy and not dependent on the NN potential model used.

Neutron-nucleus elastic scattering differential cross section and spin observable data should become available in the near future. In many cases physical effects of interest cause a large fluctuation at large angles, where it may be easier to discern such effects using neutrons rather than protons. In Figs. 10 and 11 results are shown for neutron projectile kinetic energies of 200 and 80 MeV, respectively. The effects of the medium are similar to what can be seen in Figs. 1 and 4. In Fig. 10 the medium causes the A_y to have deeper and broader minima. In Fig. 11 at $T_p = 80$ MeV the medium contribution causes larger changes, especially in the spin rotation. There is also an overall shift to larger scattering angles as is seen in Figs. 1–6.

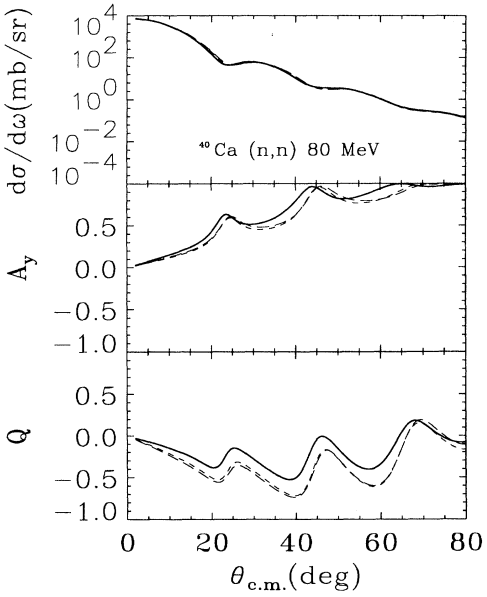

FIG. 11. The same as Fig. 1, except this is for elastic neutron-nucleus scattering at 80 MeV laboratory energy.

C. The parametric propagator energy E_i

In Eqs. (10) and (18) it was remarked that in the prescribed formalism, the energy argument for the free propagator, e, differs from the projectile energy, E, by the target nucleon single-particle energy, ε_i. In Eq. (18) the quantity $g_0(e)^{-1} - G_0(E)^{-1}$ is represented as

$$g_0(e)^{-1} - G_0(E)^{-1} = e - h_o - h_i - E + h_o + H_A$$
$$= e - E + U_i - \varepsilon_i. \quad (28)$$

In step 7 nuclear matrix elements of Eqs. (17) or (20) are taken to give eventually the optical potential. Since the formalism leading up to Eqs. (18) and (19) is designed to isolate the functional degrees of freedom describing particles o and i, while treating the remaining $A-1$ particles in an average manner, it should be reasonable to take the average mean field values of the $A-1$ pieces of the Hamiltonian in Eq. (28), i.e., letting $\varepsilon_i = -\varepsilon^i = -\langle H^i \rangle$, in spite of the fact that direct matrix elements of $\langle H^i \rangle$ are not taken in the described formalism.

With these arguments the value of E_i might be taken to be $e = E_i = E + \varepsilon_i = E - |\varepsilon_i|$, where we would like to take ε_i to be the average single-particle energy (~ -25 MeV for ^{40}Ca, although this number is model dependent). If each target nucleon single-particle state, ε_i, were to be treated individually, it is known that in the case of nucleon-nucleus scattering the more important scattering events involve the less bound target nucleons, so that the effective average ε_i would most likely lead to a smaller value of $|\varepsilon_i|$.

In the case of the free impulse approximation, excluding the medium contributions, the ideal choice of e would be to force the quantity, $g_0(e)^{-1} - G_0(E)^{-1}$ to be zero, thus providing the physically best possible representation of the medium correcting term within this context. From the first line of Eq. (28) this would involve setting

$$e - h_i - E + H_A = 0$$

or

$$e = E + \langle h_i \rangle = E + |\langle h_i \rangle|.$$

Therefore the ideal choice for e in this circumstance is to shift e by the average kinetic energy of the target nucleon, $\langle h_i \rangle$. This can be seen intuitively in that e represents the sum of the kinetic energies of particles o and i in the two-body case and so this corresponds to equating the two-body kinetic energies. This procedure in an average sense would purport to represent the effect of the medium via an energy shift. Investigations of such behavior follow. In summary for the free case the energy e should be greater than the projectile kinetic energy E by the average kinetic energy of the target nucleons, while for the cases where medium contributions are included, the energy e should be less than E by the average single-particle energy.

The shifts of the energy, e, have been shown in the case of pion-nucleus scattering to produce a significant effect on the predictions [31], where the Δ resonance causes the pion-nucleon interaction to have a large energy dependence. The free NN interaction does not have this property and has a small energy dependence, therefore the sensitivity of the nucleon-nucleus predictions to the energy shift of e should be small. This expectation has been confirmed by the rough calculation of Ref. [4].

In Figs. 12–14 results are shown for $T_p = 200$ MeV. For the free case calculations are shown with $e = 188$, 200, 212, and 224 MeV and for the DH and HFB cases, calculations with $e = 176$, 188, and 200 MeV are displayed. For the total neutron cross sections (σ_T) in Fig. 12, the increasing e causes σ_T to increase for the circles, and the decreasing e in the medium modified results decreases σ_T. Although the shift seen where the DH potential is used is larger, the overall effect is small. When compared to the medium effects as seen in Fig. 9, the energy shift can be seen to be unimportant.

For proton elastic scattering at $T_p = 200$ MeV, Fig. 13 shows the effects of shifting e for the free case, while Fig. 14 shows the shifts when the HFB mean field potential is used to represent the medium contributions. When e is decreased it can be seen that the minima are shifted to slightly larger scattering angles, and are slightly deeper. The increase of e in Fig. 13 moves the predictions away from the data, but provides only a negligible effect. The decrease of e in Fig. 14 causes better alignment of the minima, but the overall effect is very small. Similar effects are seen at other energies, although at smaller projectile energies the changes are even smaller.

The effect of the shift in e for the free case is in general to worsen the predictions when compared to the data. Also, this shift does not represent in any fashion the medium contribution effect and actually moves the predictions in the opposite direction. It can be safely said that although the energy dependence required of the NN

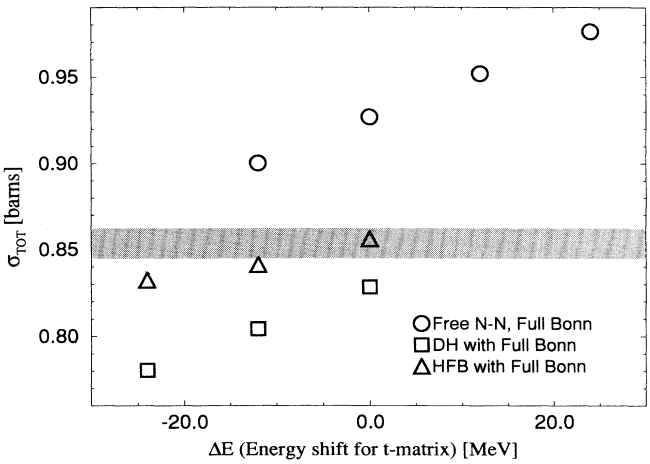

FIG. 12. The total neutron-nucleus cross section for scattering from ^{40}Ca at projectile kinetic energy, E, of 200 MeV is shown as a function of the difference between the parametric energy, e, and E, used to calculate the free NN t matrix. The circles correspond to the free result, while the squares and triangles include the medium contributions using the DH and HFB mean field potentials, respectively. The gray band corresponds to the datum and its estimated uncertainty.

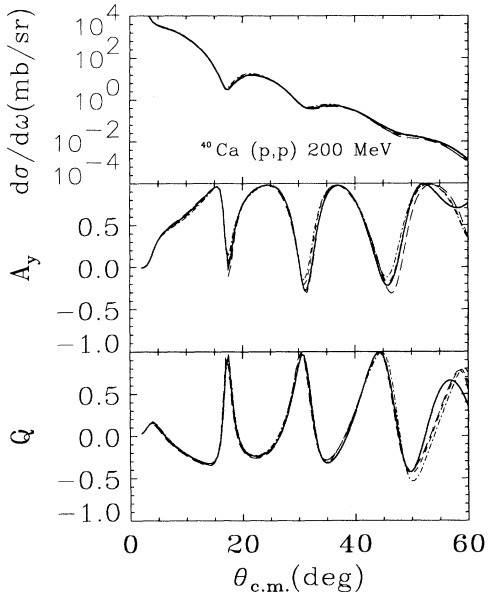

FIG. 13. The angular distribution of the differential cross section ($\frac{d\sigma}{d\Omega}$), analyzing power (A_y), and spin rotation function (Q) for elastic proton scattering from ^{40}Ca at 200 MeV laboratory energy. The results are shown for the free case with no medium corrections included. The parametric energy, e, used for the free NN t matrix calculation is set to be equal to 200, 188, 212, and 224 MeV for the solid, short-dashed, long-dashed, and dot-dashed curves, respectively.

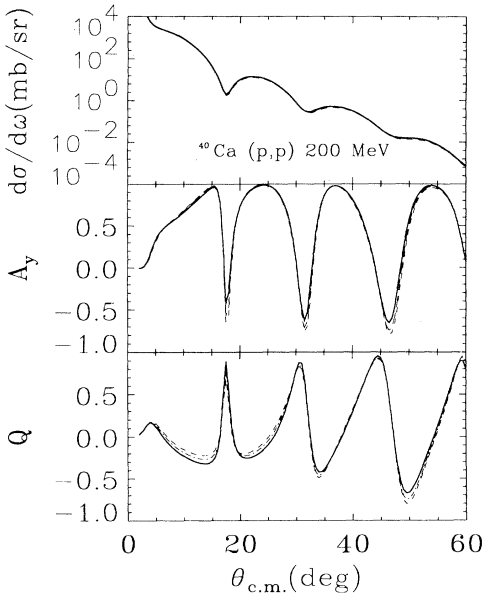

FIG. 14. The angular distribution of the differential cross section ($\frac{d\sigma}{d\Omega}$), analyzing power (A_y), and spin rotation function (Q) for elastic proton scattering from ^{40}Ca at 200 MeV laboratory energy. The results are shown where the medium contributions are included using the HFB mean field potential. The parametric energy, e, used for the free NN t matrix is set to be equal to 200, 188, and 176 MeV for the solid, short-dashed, and long-dashed curves, respectively.

effective t matrix favors including the medium contributions, this dependence can be neglected.

IV. SUMMARY AND CONCLUSION

Although the impulse approximation to the optical potential, which uses the free NN t matrix to represent the interaction between the projectile and the target nucleon, has been highly successful, the effects associated with the interaction between the target nucleon and the residual nucleus have not been clearly delineated. The spectator expansion of multiple scattering theory requires an effective NN interaction, which differs from the free NN interaction in that the implied many-body propagator corresponds to the free propagation of the projectile through the nuclear medium. A systematic formalism is developed in this paper, consistent with multiple scattering theory and the spectator expansion, where a mean field potential, representing the action of the residual nucleus upon the target nucleon, is used to model the medium contributions, which correspond to the difference between the effective and the free NN interaction. This formalism is straightforward, thus providing a much clearer and precise interpretation of the effects of the medium than had existed in the past, and likewise providing an unambiguous basis for later inclusion of higher-order effects.

Calculations have been performed with two mean field potentials, taken from realistic and proven microscopic nuclear structure models to represent the medium contribution. The full spin structure of the mean field potential and the free NN t matrix is included along with the off-shell and nonlocal effects. Results demonstrate that the medium contributions consistently provide a significant, non-negligible improvement in the predictions of the data in the case of elastic nucleon-nucleus scattering from ^{40}Ca at projectile kinetic energies between 48 and 200 MeV. Above 200 MeV the medium effect is insignificant at scattering angles less than $\sim 40°$.

ACKNOWLEDGMENTS

One of the authors (C.R.C.) would like to acknowledge the gracious hospitality of the Service de Physique et Techniques Nucléaires at the Centre d'Etudes de Bruyères-le-Châtel, where part of this work was performed. Discussions with B. Giraud and the computational support of the Ohio Supercomputer Center under Grant Nos. PHS206 and PDS150 are gratefully acknowledged. This work was performed in part under the auspices of the U.S. Department of Energy under Contract Nos. DE-FG02-93ER40756 with Ohio University, DE-AC05-84OR21400 with Martin Marietta Energy Systems, Inc., and DE-FG05-87ER40376 with Vanderbilt University. This research was supported in part by the U.S. Department of Energy, Office of Scientific Computing under the High Performance Computing and Communications Program (HPCC) as a Grand Challenge titled the Quantum Structure of Matter.

[1] R. Crespo, R. C. Johnson, and J. A. Tostevin, Phys. Rev. C **41**, 2257 (1990).
[2] H. F. Arellano, F. A. Brieva, and W. G. Love, Phys. Rev. Lett. **63**, 605 (1989); Phys. Rev. C **41**, 2188 (1990).
[3] Ch. Elster, T. Cheon, E. F. Redish, and P. C. Tandy, Phys. Rev. C **41**, 814 (1990).
[4] R. Crespo, R. C. Johnson, and J. A. Tostevin, Phys. Rev. C **48**, 351 (1993).
[5] C. R. Chinn, Ch. Elster, and R. M. Thaler, Phys. Rev. C **44**, 1569 (1991).
[6] L-C. Liu, Ch. Elster, and R. M. Thaler, J. Phys. G (to be published).
[7] R. Crespo, R. C. Johnson, and J. A. Tostevin, Phys. Rev. C **44**, R1735 (1991); *ibid.* **46**, 279 (1992).
[8] H. F. Arellano and W. G. Love, Phys. Rev. C **45**, 759 (1992).
[9] C. R. Chinn, Ch. Elster, and R. M. Thaler, Phys. Rev. C **47**, 2242 (1993).
[10] K. M. Watson, Phys. Rev. **89**, 575 (1953); N. C. Francis and K. M. Watson, *ibid.* **92**, 291 (1953).
[11] A. Kerman, M. McManus, and R. M. Thaler, Ann. Phys. **8**, 551 (1959).
[12] A. Picklesimer and R. M. Thaler, Phys. Rev. C **23**, 42 (1981).
[13] E. R. Siciliano and R. M. Thaler, Phys. Rev. C **16**, 1322 (1977).
[14] H. Garcilazo and W. R. Gibbs, Nucl. Phys. **A356**, 284 (1981); K. A. Kabir, M. Silver, and N. Austern, Phys. Rev. C **27**, 2104 (1983).
[15] P. C. Tandy, E. F. Redish, and D. Bollé, Phys. Rev. C **16**, 1924 (1977).
[16] K. L. Kowalski and A. Picklesimer, Nucl. Phys. **A369**, 336 (1981); Ann. Phys. (N.Y.) **139**, 215 (1982).
[17] G. Takeda and K. M. Watson, Phys. Rev. **97**, 1336 (1955).
[18] F. A. Brieva and J. R. Rook, Nucl. Phys. **A291**, 299 (1977); **A291**, 317 (1977); **A297**, 206 (1978); **A307**, 493 (1978).
[19] L. Ray, G. W. Hoffman, and W. R. Coker, Phys. Rep. **212**, 223 (1992), and references contained within.
[20] P. Ring and P. Schuck, *The Nuclear Many-Body Problem* (Springer-Verlag, New York, 1980).
[21] See, for example, J. F. Berger, M. Girod, and D. Gogny, Nucl. Phys. **A502**, 85c (1989); J. P. Delaroche, M. Girod, J. Libert, and I. Deloncle, Phys. Lett. B **232**, 145 (1989).
[22] J. F. Berger, M. Girod, and D. Gogny, Comput. Phys. Commun. **63**, 365 (1991).
[23] C. J. Horowitz and B. D. Serot, Nucl. Phys **A368**, 503 (1981).
[24] R. Machleidt, K. Holinde, and Ch. Elster, Phys. Rep. **149**, 1 (1987).
[25] Ch. Elster and P. C. Tandy, Phys. Rev. C **40**, 881 (1989).
[26] M. Jacob and G. C. Wick, Ann. Phys. (N.Y.) **7**, 404 (1959).
[27] A. Picklesimer, P. C. Tandy, R. M. Thaler, and D. H. Wolfe, Phys. Rev. C **30**, 2225 (1984).
[28] I. Sick, J. B. Bellicard, J. M. Cavedon, B. Frois, M. Huet, P. Leconte, P. X. Ho, and S. Platchkov, Phys. Lett. **88B**, 245 (1979).
[29] R. W. Finlay, W. P. Abfalterer, G. Fink, E. Montei, T. Adami, P. W. Lisowski, G. L. Morgan, and R. C. Haight, Phys. Rev. C **47**, 237 (1993).
[30] R. W. Finlay, G. Fink, W. Abfalterer, P. Lisowski, G. L. Morgan, and R. C. Haight, in *Proceedings of the International Conference on Nuclear Data for Science and Technology*, edited by S. M. Qain (Springer-Verlag, Berlin, 1992), p. 720.
[31] D. J. Ernst and M. B. Johnson, Phys. Rev. C **32**, 940 (1985); D. J. Ernst, D. R. Giebink, and M. B. Johnson, Phys. Lett. B **182**, 242 (1986).
[32] J. Kelly, in *Polarization Phenomena in Nuclear Physics–1980 (Fifth International Symposium, Santa Fe),* Proceedings of the Fifth International Symposium on Polarization Phenomena in Nuclear Physics, AIP Conf. Proc. No. 69, edited by G. G. Ohlson, R. E. Brown, N. Jarmie, W. W. McNaughton, and G. M. Hale (AIP, New York, 1981), p. 454; E.J. Stephenson, *Antinucleon- and Nucleon-Nucleus Interaction*, edited by G. Walker, C. D. Goodman, and C. Olmer (Plenum, New York, 1985), p. 299.
[33] P. Schwandt, H. O. Meyer, W. W. Jacobs, A. D. Bacher, S. E. Vigdor, and M. D. Kaitchuck, Phys. Rev. C **26**, 55 (1982); A. Nadasen, P. Schwandt, P. P. Singh, W. W. Jacobs, A. D. Bacher, P. T. Debevec, M. D. Kaitchuch, and J. T. Meek, Phys. Rev. C **23**, 1023 (1981).
[34] H. Seifert, Ph.D. thesis, University of Maryland, 1990.
[35] H. Sakaguchi, M. Nakamura, K. Hatanaka, A. Goto, T. Noro, F. Ohtani, H. Sakamoto, H. Ogawa, and S. Kobayashi, Phys. Rev. C **26**, 944 (1982).
[36] R. H. McCamis *et al.*, Phys. Rev. C **33**, 1624 (1986); K. H. Bray, K. S. Jayaraman, G. A. Moss, W. T. H. Oers, D. O. Wells, and Y. I. Wu, Nucl. Phys. **A167**, 57 (1971).